Proceedings of the International Symposium on Managed Aquifer Recharge (ISMAR 10)

Managed Aquifer Recharge: Local solutions to the global water crisis

GrupoTragsa
Garantía Profesional. Servicio Público

Subdirección de Innovación y Desarrollo de Servicios

Author: Multiauthor
ISBN-13: 978-84-09-15736-5

Empresa de Transformación Agraria, S.A. (TRAGSA)
C/ Maldonado, 58
28006 Madrid Spain

Editor:
Enrique Fernández Escalante. Dr. in hydrogeology, Innovation Subdirectorate, Tragsa Group.

Editorial team:
Jon San Sebastián Sauto. Dr. in Biology, Tragsatec.
Rodrigo Calero Gil. Agronomic Engineer. Innovation Subdirectorate, Tragsa Group.
Rocío Ortega Labrandero Agronomic Engineer. Innovation Subdirectorate, Tragsa Group.
José Antonio de la Orden. Dr. Minning Engeneer. Instituto Geológico y Minero de España.

Madrid, 2019, November

Topic 8. SUSTAINABLE MAR TECHNICAL SOLUTIONS

Paper for ISMAR10 symposium. *Topic No: 8 (025#)*

Dipolic MAR "Bubble" Inside Confined Brine Formation or Floating "Lens" on Top of Unconfined Saline Aquifer

Anvar Kacimov[1*], Yurii Obnosov[2] and Ali Al-Maktoumi[1]

1. Sultan Qaboos University, Oman; anvar@squ.edu.om, ali4530@squ.edu.om
2. Kazan Federal University Russia; yobnosov@kpfu.ru
*Correspondence: anvar@squ.edu.om; Tel.: (968) 99251302

Abstract: In arid desert environments, MAR sites are often characterized by high salinity of the ambient groundwater and intensive evaporation. We present mathematical modeling of two MAR scenarios: 1) injection-abstraction of fresh water through two horizontal wells with a quasi-vertical sharp interface/transition zone straddling between the caprock and bedrock of a confined aquifer; 2) infiltration from a surface pond into a floating fresh water lens with an interface pinned to two unknown frontal points. Analytical solutions for Darcian, steady, 2-D and axisymmetric flows utilize two types of mathematical dipoles: combination of a line sink and source and superposition of a distributed sink and source. For 2-D dipoles sandwiched between the caprock and bedrock, the theory of holomorphic functions is used (conformal mappings and Keldysh–Sedov's representations of characteristic functions via singular integrals). Numerically, MODFLOW-SEAWAT delineate isoconcentric lines of the MAR "bubble". For axisymmetric floating lenses, U-turn topology of fresh water circulation is modeled by the Dupuit-Forchheimer approximation, which is reduced to a boundary value problem for a nonlinear ordinary differential equation with respect to Strack's potential. The total volume of the lens is evaluated for evaporation rates, which are constant or exponentially decrease with the water table depth.

Keywords: Abstraction-injection wells; isoconcentric lines; sharp interface; density dependent flow; fresh water "bubble"; floating fresh water lens; evaporation from the water; analytical and numerical solutions.

1. Introduction

ASR in deserts of Central Asia, in particular, in Turkmenistan, has been traditionally practiced by local nomads who constructed the so-called "takyrs" (natural topographic depressions with dug wells) [1]. Runoff was collected in these infiltration basins during rainy seasons and infiltrated to an unconfined aquifer through a usually silt-clogged bed. Later on, old "takyrs" were amended by bulldozed excavations and systems of injection-abstraction wells [6,9], which currently supply water to towns, industries and large-scale irrigated agriculture in the desert. The created "perched" pore-water bodies in these ASR schemes belong to the class of

terrestrial freshwater lenses [7], which are subtended by high-salinity "pristine" groundwater. A smart recovery of the stored rainwater from the "floating lens" is necessary to thwart overpumping-upconing. The "takyr" lenses have the following peculiarity: the phreatic surface is often shallow and the lens intensively evaporates and transpires (lash desert vegetation emerges on the ground surface over a MAR-generated lens) that causes dwindling-extermination of the lens if infiltration stops.

In this paper, we present analytical modeling of two MAR schemes:

In Section 2, we extend our idea of ASR by a dipole of horizontal wells [3]. In order to avoid evaporation and secondary salinization of the topsoil, a fresh pore-water "bubble" is confined by the caprock of a confined aquifer containing saline groundwater.

In Section 3, we investigate a "takyr" lens in an unconfined aquifer with saline water and nontrivial evapotranspiration from the water table.

2. MAR "bubble" generated by dipole sandwiched in confined aquifer

We consider a confined aquifer of a given thickness b, with a horizontal impervious caprock B_1B_2 and bedrock G_1G_2 (Fig.1a). The case of a half-plane i.e. deep bedrock ($b=\infty$) has been studied in [3].

Saline groundwater of density ρ_s is stagnant and, if no MAR, occupies the whole strip of Fig.1a. The dipole (a pair of injection-abstraction wells located a small distance $2j$ from each other) of intensity $2q$, is located at the depth $y=-h_1$ and creates a fresh water "bubble" (density of fresh water is ρ_f), which is laterally bounded by the interfaces E_2A_2 and E_1A_1. The piezometric head in saline water, h_{sa}, is counted from Nx. At a certain point B far away from the "bubble" in Fig.1a the pressure head in a hypothetical piezometer tapping saline water is p_B.

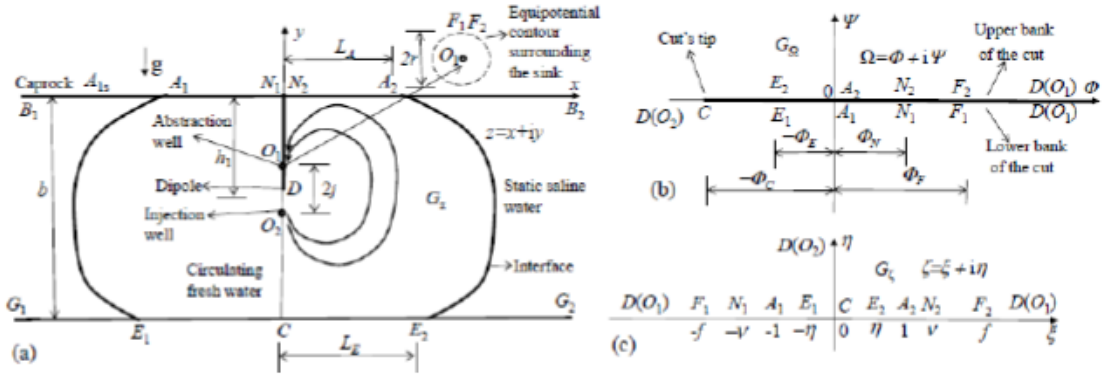

Figure 1. Vertical cross-section of the fresh-water lens generated by 2-D dipole in a confined aquifer (a), complex potential domain (b), reference plane (c).

We assume that the contours of the wells in the dipole are circles of a small radius r surrounding the sink and source. The pressure head at points F_1, F_2 (the apex of the abstraction well contour) is p_F (see a hypothetical piezometer zoomed in Fig.1a).We introduce a complex physical coordinate $z=x+\mathrm{i}\,y$, velocity potential $\Phi=-kh_f$ of the moving fresh water and the complex potential $\Omega=\Phi+\mathrm{i}\Psi$, where $h_f(x,y)$ is the hydraulic head in the fresh water, Ψ is a stream function and k is a given saturated fresh water conductivity. The specific discharge vector is $\vec{V}=\nabla\Phi$. The pressure and pressure head in fresh water are $P_f=\rho_f g p_f$ and $p_f(x,y)=-(\Phi/k+y+c_p)$, respectively. We select points A_2 and A_1 (Fig.1a) as fiducial i.e. $\Omega(A_1)=\Omega(A_2)=0$. Then $c_p=-\rho_s/\rho_f p_B$. The pressure and pressure head in saline water are

$P_s = \rho_s g p_s$, and $p_s(y) = p_B - y$. Along the two interfaces in Fig.1a the free boundary conditions are:

$$\Phi - cy = 0, \quad \Psi = 0, \tag{1}$$

where $c = (\rho_s / \rho_f - 1)k$ [10,12].

At points N_1 (N_2), F_1 (F_2), E_1(E_2), C the velocity potentials are $\Phi_N, \Phi_F, \Phi_E,$ and $-\Phi_C$, correspondingly. Point F_1 (F_2) is the apex of the abstraction well (a circular equipotential). The complex potential domain G_Ω is a plane with a horizontal cut (Fig.1b).

We map G_Ω onto the upper half-plane G_ζ of an auxiliary reference complex variable $\zeta = \xi + \mathrm{i}\eta$ (Fig.1c) by the function:

$$\begin{aligned} &\Omega = \Phi_C(\zeta^2 - 1), \quad (0,1,\infty) \to (-\Phi_C, 0, \infty), \\ &\Phi_N = \Phi_C(\nu^2 - 1), \quad \Phi_F = \Phi_C(f^2 - 1), \quad \Phi_E = \Phi_C(1 - \eta^2). \end{aligned} \tag{2}$$

Taking into account eqn.(2), the holomorphic function $z(\zeta)$ satisfies the following boundary conditions:

$$\begin{aligned} &x(\xi) = 0, \qquad \xi \in (-\infty, -\nu) \cup (\nu, \infty), \\ &y(\xi) = 0, \qquad \xi \in (-\nu, -1) \cup (1, \nu), \\ &y(\xi) = \Phi(\xi)/c = \Phi_C(\xi^2 - 1)/c, \qquad \xi \in (-1, -\eta) \cup (\eta, 1), \\ &y(\xi) = -b, \qquad \xi \in (-\eta, \eta). \end{aligned} \tag{3}$$

Solution to the mixed boundary-value problem (3) is bounded at infinity and at all transition points: $\pm\nu$, ± 1, $\pm\eta$. The last condition is satisfied if and only if $\Phi_C(1 - \eta^2) = cb$. The Keldysh-Sedov formula [2] gives, after simple transformations, the required solution to problem (3):

$$z(\zeta) = \frac{2\zeta\sqrt{\nu^2 - \zeta^2}}{\pi}\left[\frac{\Phi_C}{c}\int_\eta^1 \frac{\tau^2 - 1}{\sqrt{\nu^2 - \tau^2}}\frac{\mathrm{d}\tau}{\tau^2 - \zeta^2} + \int_0^\eta \frac{b}{\sqrt{\nu^2 - \tau^2}}\frac{\mathrm{d}\tau}{\tau^2 - \zeta^2}\right]. \tag{4}$$

We introduce dimensionless quantities $(z_d, x_d, y_d, r_d, b_d,) = (z, x, y, r, b)/h_1$ $(\Phi_{Fd}, \Phi_{Cd}, \Phi_{Ed}, \Phi_{Ad}, \Omega_d) = (\Phi_F, \Phi_C, \Phi_E, \Phi_A, \Omega)/(kh_1)$, $\delta = \rho_s / \rho_f - 1$. If the parameters c, b, r, Φ_F are fixed, then from the condition of solvability and the corresponding relation (2) it follows:

$$\eta = \sqrt{1 - b\delta(f^2 - 1)/\Phi_F}, \tag{5}$$

that implies the inequality $b\delta(f^2 - 1) < \Phi_F$. From the condition: $z(\infty) = -\mathrm{i}$ (the dipole is placed at a given depth h_1 under the caprock) and $z(f) = -\mathrm{i}(1 - r)$ (the apex of the contour of the abstraction well, point $F_{1,2}$ is at an elevation r above the sink) we obtain

$$\nu = \sqrt{1 + \frac{4}{\pi^2}\left[\frac{\Phi_F}{3\delta(f^2 - 1)}\left(\eta^3 - 3\eta + 2\right) - b\eta\right]^2}, \tag{6}$$

$$1-r=\frac{2f\sqrt{f^2-\nu^2}}{\pi}\left[\frac{\Phi_F}{(f^2-1)\delta}\int_\eta^1\frac{\tau^2-1}{\sqrt{\nu^2-\tau^2}}\frac{\mathrm{d}\tau}{\tau^2-f^2}+\int_0^\eta\frac{b}{\sqrt{\nu^2-\tau^2}}\frac{\mathrm{d}\tau}{\tau^2-f^2}\right]. \quad (7)$$

The system of three nonlinear equations (5)-(7) with respect to η, f, ν is reduced to a single equation with respect to f. We solved this equation by the **FindRoot routine** [13]. Then, similarly to [3], we used eqns. (2) and (4) and computed the shapes of the bubble.

A finite difference variable-density, saturated groundwater flow and transport code, SEAWAT [8] has been also used to simulate the problem presented in Fig.2 which depicts a vertical cross section of a homogeneous isotropic aquifer having k= 10 m/day, porosity 0.25 and thickness b=10 m. The modeled domain is 30 m wide. It was gridded with 100 layers and 300 columns forming a total number of 30,000 active cells with the cell size dy=dx =0.1 m. The longitudinal dispersivity, αL, and the molecular diffusion coefficient, D_0, were 10 m and 1×10^{-10} m²/day, respectively. The initial concentration of solutes in groundwater across the aquifer is 35 g/L. The fluid density and solute concentration were linearly related to a factor of 0.7. At the time instance t= 0, the abstraction and injection wells started their operation by pumping at equal rates of 1600 m³/day. Four sides of the rectangle in Fig. 2 are assumed impermeable to both flow and transport. Simulations continued with t until a steady state has been reached. The isoconcentric lines and the equipotential lines are presented in Fig.2.

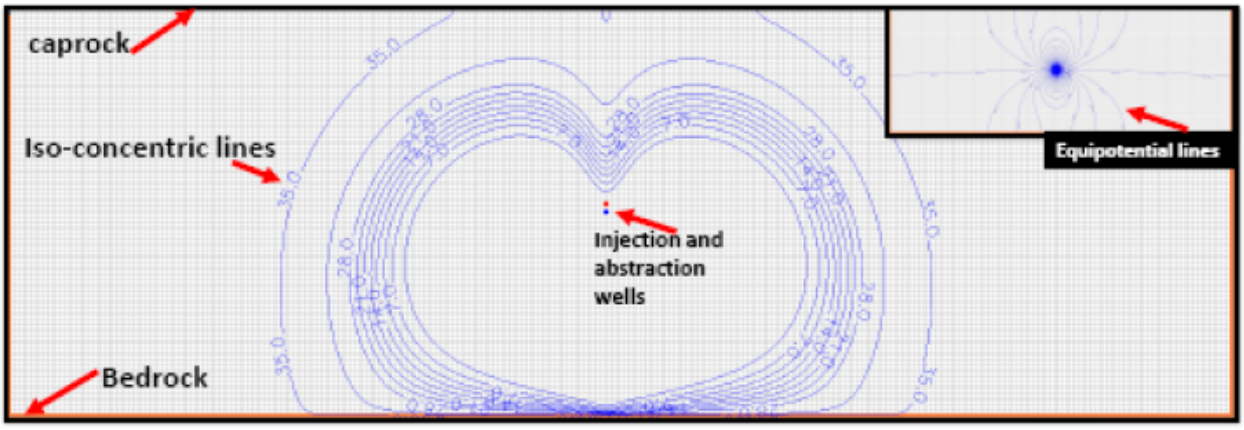

Figure 2.

Similarly to [3], the isoconcentric lines are downconing towards the upper abstraction well but the bedrock facilitates "bubble's" confinement.

3. Floating lens under infiltrating "takyr" in unconfined aquifer

A circular infiltration basin of a radius R_M^* has an average ponding depth H^* (Fig.3). The clogging layer (cake) has a thickness s and hydraulic conductivity k_c. A volume V_0 of runoff is collected and infiltrated in T^* days through the vadose zone into the lens beneath. A steady-state infiltration rate $N_0^* \approx Hk_c / s$ is not impeded by the mounding phreatic surface located well below the cake bottom. Prior to MAR, saline groundwater has a horizontal water table at the depth d_0^* under the desert surface.

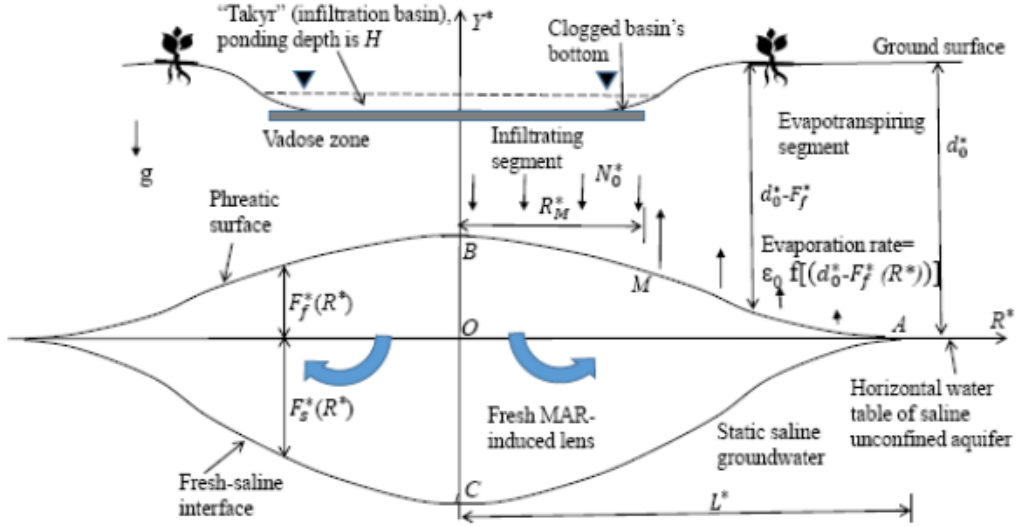

Figure 3.

Evapotranspiration (usually ignored in MAR models) is a key hydrological driver which maintains a stationary un-pumped desert lens subtended by saline static groundwater [4]. There is no abstraction (recovery) from the lens in Fig.3. Flow is axisymmetric and we consider one half of the axial cross section. A sharp interface *CA* in Fig.3 is a "magnified replica" of an *apriori* unknown phreatic surface *BMA*, along which the sink-source boundary conditions are similar to ones on the top of a Tothian "unit basin" [13], usually assumed to be a fixed rectangle or trapezium. In other words, unlike the flow domains in [13] ours is bounded by two free surfaces and none of the characteristic points (*B*,*M*, or *A*) are *apriori* known.

Along the segment *BM* of the phreatic surface the lens is recharged and along *MA* natural evapotranspiration discharges fresh water back into the vadose zone-atmosphere. The intensity of evaporation depends on the depth of *MA* under the ground surface according to the following relation:

$$\varepsilon = \varepsilon_0^* f(d_0^* - F_f^*[R^*]), \tag{8}$$

where ε_0^* is a given evaporation rate from a saturated ground surface (taken from, say, the FAO/Penman-Monteith formula) and *f* is a dimensionless function, which reflects experimentally measured decrease of evaporation from the water table with the increase of its depth. For simplicity of mathematical modeling, in [3] and [10] "trivial" regimes of a constant *f* and *f* linearly decreasing with the water table depth have been studied. Below, we adopt the model from [5], where experimental data for exponential relation in eqn.(8) have been reported.

The locus of point A (the tip of the lens) is a part of solution. The volume V_f^* of fresh water in the lens (a body of revolution) is a design parameter. We select cylindrical coordinates (*OR**Y*). The height of the water table above the reference plane Y*=0 is $F_f^*(R^*)$. The depth of the interface is $F_s^*(R^*)$.

We use the Dupuit-Forchheimer model (see e.g. [10,12] for details) for flow inside the lens that yields an ODE

$$\frac{1}{R^*}\frac{\mathrm{d}}{\mathrm{d}R^*}\left(R^* k\,(F_f^* + F_s^*)\frac{\mathrm{d}F_f^*}{\mathrm{d}R^*}\right) = \begin{cases} -N_0^*, & 0 \le R^* \le R_M^*, \\ \varepsilon_0^* f(d_0^* - F_f^*[R^*]), & R_M^* \le R^* \le L^*. \end{cases} \tag{9}$$

We select an evaporation function:

$$\varepsilon = \varepsilon_0^* \exp(-\alpha^*(d_0^* - F_f^{*2}[R^*])), \tag{10}$$

where α^* (1/m) is a given constant which quantifies the decay of evaporation with depth.

According to the Ghijben-Herzberg relation [10,12] the height of the water table and depth of the interface are related as:

$$F_s^* = F_f^* / \gamma, \quad \gamma = (\rho_s - \rho_f)/\rho_s. \tag{11}$$

We introduce dimensionless quantities:

$$(F_s, F_f, R, Y, R_M, L, d, d_0) = (F_s^*, F_f^*, R^*, Y^*, R^*_M, L^*, d^*, d^*_0)/\forall_0^{1/3},$$

$$\varepsilon_0 = \varepsilon_0^*/k, \;\; N_0 = N_0^*/k, V_f = V_f^*/V_0, T = T^* k/V_0^{1/3}, \alpha = \alpha^* V_0^{1/3}, \beta = 1/\sqrt{T\pi}, R_M = \beta/\sqrt{N_0}$$

Then eqn.(9) reads:

$$\frac{\gamma}{1+\gamma}\frac{1}{R}\frac{\mathrm{d}}{\mathrm{d}R}\left[R\,F_f\frac{\mathrm{d}F_f}{\mathrm{d}R}\right] = \begin{cases} -N_0, & 0 \le R \le R_M, \\ \varepsilon_0 \exp(-\alpha(d_0 - F_f^2[R])), & R_M \le R \le L, \end{cases} \tag{12}$$

The following boundary conditions are:

$$F_f'(0) = 0, \quad F_f(L) = 0. \tag{13}$$

They reflect field observations of "takyr" lenses [6] which are indeed symmetric and taper towards point *A* in Fig.3.

By integrating eqn. (12) over the interval $(0, R_M)$ under the first condition (13), we obtain

$$F_f(R) = \sqrt{c - \frac{N_0(1+\gamma)}{2\gamma}R^2}, \tag{14}$$

where *c* is an unknown integration parameter (the apex of the MAR groundwater mound). A trivial "ellipsoidal cap" (14) appears due to linearity of eqn.(12) with respect to Strack's comprehensive potential [11]. Along the interval (R_M, L), eqn.(12) is a nonlinear second-order ODE with two boundary conditions:

$$F_f(R_M) = \sqrt{c - 0.5N_0(1+1/\gamma)R_M^2}, \; F_f(L) = 0. \tag{15}$$

The boundary-value problem (12), (15) has to be solved in a domain of an unknown width $L - R_M$ and with a boundary condition at the left edge, which depends on *c* i.e. the elevation of point *B* (Fig.3), the apex of the "ellipsoidal "cap" of the lens. In this manner, the infiltrating centre of the lens is conjugated with its evapotranspiring "periphery".

The value of *L* is found from conservation of mass:

$$N_0 R_M^2 = 2\varepsilon_0 \int_{R_M}^{L} \exp[-\alpha(d_0 - F_f^2(R))] R\,\mathrm{d}R. \tag{16}$$

Eqn.(16) states that all water which enters the lens through an infiltration disk (bounded by *BM* in the axial cross-section of Fig.3) makes a U-turn and exfiltrates/evapotranspires through the annular zone (bounded by *MA*), exactly as the Toth model [13] stipulates. The volume of fresh water in the lens is:

$$V_f = 2\pi(1+1/\gamma)\int_0^L r\,F_f(r)\mathrm{d}r.$$

We used *Mathematica* routines NDSolve and NIntegrate [14] to solve the boundary-value problem (12)-(16).

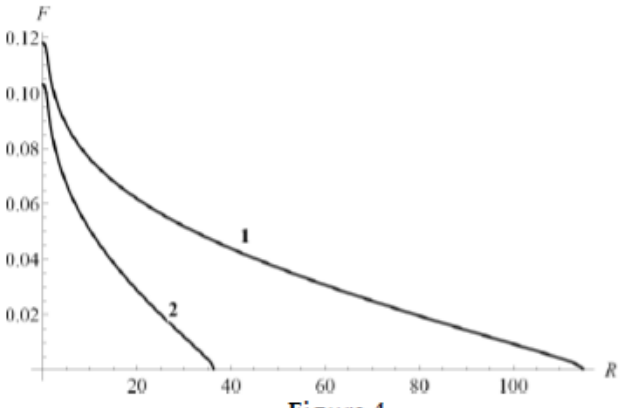

Figure 4

Figure 4 shows the computed water table for d_0=1, N_0 =0.1, $\alpha = 5$, β =0.316 (R_M =1), γ =0.03 and ε_0=0.001 and 0.01 (curves 1-2, correspondingly). The radii L of the "takyrs" in Fig.4 are 114.8 and 36.5, the fresh water volumes V_f are 32520 and 3256 i.e. significantly reduced by increased evaporation, although the apex B dropped less than 20%.

4. Discussion

In saline confined aquifers of arid deserts, a new technology of MAR by continuous injection-abstraction of fresh water into a confined (i.e. evaporation-protected) aquifer is proposed. Pore water circulates in a "bubble" vertically squeezed by a caprock and bedrock and laterally bounded by sharp interfaces demarcating a heavy and static groundwater. Mathematically, this problem is similar to another (traditional) MAR scheme: infiltration of fresh water from a surface basin into a fresh water lens which "floats" on saline groundwater [6]. We developed two conceptual models and obtained new analytical and numerical solutions for potential 2-D and axisymmetric Dupuit-Forchheimer flows and solute transport in the "bubble" and lens. In particular, we found the sizes of MAR-generated fresh water zones. Phreatic surfaces, sharp interfaces or transition zones between waters of contrasting density-salinity are delineated. It is noteworthy that steady state flow of fresh pore water is maintained by a continuous action of an intricately commingled hydrodynamic dyad (source and sink, either linear or distributed). Without a sink (abstraction well or evapotranspiration) a steady lens or "bubble" do not exist. Our solutions answer several pending questions [6,7] on mechanisms of MAR in desert oasis lenses, viz. how the sizes of the fresh water entities depend on the density contrast of the two waters, infiltration-evaporation or injection-abstraction rates and geometrical parameters of the corresponding dipole schemes. Analytical and numerical tools can be also used for optimization of characteristics of the "bubbles" and lenses, e.g. the lens storage V_f can be maximized by varying the basin sizes R_M and infiltration rate N (proportional to the depth of water in the "takyr").

Acknowledgments: This work was supported by SQU, grant IG/CAMS/SWAE/18/01. The cost to publish in open access is not covered by this grant.

Author Contributions: A.K. and Yu.O. developed analytical solutions; A.A-M. obtained numerical solutions; all three authors wrote the paper.

Conflicts of Interest: The authors declare no conflict of interest.

Abbreviations:
The following abbreviations are used in this manuscript:
ASR: Aquifer storage and recovery
MAR: Managed aquifer recharge.

References

1. Babaev A.G. (ed.), 1999. Desert Problems and Desertification in Central Asia: The Researches of the Desert Institute, Springer, Berlin.
2. Henrici, P., 1993. Applied and Computational Complex Analysis. Volume 3: Discrete Fourier Analysis, Cauchy Integrals, Construction of Conformal Maps, Univalent Functions. Wiley. New York.
3. Kacimov, A., Obnosov, Yu.V., and Al-Maktoumi, A., 2018. Dipolic flows relevant to aquifer storage and recovery: Strack's sink solution revisited. Transport in Porous Media, 123(1), 21–44.
4. Kacimov, A. and Obnosov, Yu.V., 2019. Analytic solutions for infiltration-evaporation formed fresh groundwater lenses floating on saline water table under desert dunes: Kunin-Van Der Veer legacy revisited. Submitted to J. of Hydrology (revised version under review).
5. Katz, D.M., 1968. The regularities of ground water evaporation in irrigation lands of the arid zone. Water in the Unsaturated Zone, IAHS Symposium, Wageningen, 822-827.
6. Kunin, V.N., 1959. Local Waters in Deserts and Problems in Their Utilization. Akad. Nauk SSSR, Moscow (in Russian).
7. Laattoe, T., Werner, A.D., Woods, J.A. and Cartwright, I., 2017. Terrestrial freshwater lenses: Unexplored subterranean oases. J. of Hydrology, 553, 501-507.
8. Langevin, C.D., Thorne Jr., D.T., Dausman, A.M., Sukop, M.C, and Guo, W., 2008. SEAWAT Version 4: A Computer Program for Simulation of Multi-Species Solute and Heat Transport. Techniques and Methods Book 6, Chapter A22. U.S. Geological Survey.
9. Platonov, A.A., 1934. Takyr. Krasnaya Nov', 9, 82–93 (in Russian).
10. Polubarinova-Kochina, P.Ya., 1977. Theory of Ground Water Movement. Nauka, Moscow (in Russian).
11. Strack, O.D.L., 1978. Distributed sources for unconfined groundwater flow in a half-space. J. of Hydrology, 39, 239-253.
12. Strack, O.D.L., 2017. Analytical Groundwater Mechanics. Cambridge Univ. Press, New York.
13. Tóth, J., 2009. Gravitational Systems of Groundwater Flow: Theory, Evaluation, Utilization. Cambridge Univ. Press., New York.
14. Wolfram, S., 1991. Mathematica. A System for Doing Mathematics by Computer. Addison-Wesley, Redwood City.